Desalination and Water Treatment
www.deswater.com

doi: 10.5004/dwt.2019.23810

151 (2019) 332–341
May

Two-stage cubature Kalman filter and its application in water pollution modeling

Lu Zhang[a,*], Yongfei Miao[b], Hailun Wang[a], Jianwen Fang[a]

[a]*School of Electrical and Information Engineering, Quzhou University, Zhejiang, China, emails: zhanglu@qzc.edu.cn (L. Zhang), wanghailun@qzc.edu.cn (H. Wang), fangjianwen@qzc.edu.cn (J. Fang),*
[b]*Department of Radio Navigation,Dalian Air Force Sergeant School of Communication, Dalian, Liaoning, 116600, email: yongfei1900@163.com*

Received 20 January 2018; Accepted 20 January 2019

ABSTRACT

Water pollution models are generally nonlinear systems that incorporate some random bias. The most common modeling method is to use an augmented-state cubature Kalman filter, although the computational requirements of this approach can be excessive. In this paper, a two-stage cubature Kalman filter is proposed to overcome this problem. The estimates given by the two-stage cubature Kalman filter can be expressed as the output of an advanced bias-free filter and a bias filter. The two-stage cubature Kalman filter is equivalent to the augmented-state cubature Kalman filter in terms of accuracy, but with a much smaller computational load. Simulation results demonstrate the validity of the two-stage cubature Kalman filter for water pollution modeling, and prove the equivalence of the two algorithms.

Keywords: Two-stage cubature Kalman filter; Water pollution model; Nonlinear system; Random bias

1. Introduction

For problems involving nonlinear systems with random bias, a common approach is to use an augmented-state cubature Kalman filter (CKF), which treats the bias as part of the state, i.e., the state is estimated as well as the bias. As the complexity of a system increases in practical applications, the computational load of the augmented-state CKF will dramatically increase. This can easily cause overflows and failures when running models on digital computers. To avoid the need for the augmented-state CKF, researchers have proposed a two-stage filtering method. Friedland proposed a two-stage filter in which a bias-free filter operates in parallel with a bias filter. Although, this method is optimal for constant bias, it is suboptimal for random bias unless suitable algebraic constraints exist [1,2]. Hsieh and Keller have proposed an optimal two-stage Kalman estimator that extends Friedland's estimator and is optimal in general conditions [3,4]. Many other researchers have contributed in this area, leading Hsieh to present a general two-stage Kalman filter that provides the optimal estimate of the system state and can be applied to general, time-varying and linear dynamic systems [5]. The new filter reduces the computational complexity of models involving random bias.

In practical applications, nonlinear filter techniques are often required [6–8]. Hsieh extended the linear general two-stage filter to nonlinear systems and proposed a general two-stage extended Kalman filter that is mathematically equivalent to the extended Kalman filter [9]. Zhang et al. [10–13] proposed a new third-degree adaptive extended CKF algorithm, a novel class of interpolatory CKFs, a high-order unscented Kalman filtering method, and a quasi-stochastic integration filter. Xu et al. [14] presented a two-stage unscented Kalman filter that uses a forgetting

* Corresponding author.

factor to compensate for the effects of incomplete information. Chen et al. [15] proposed a novel two-stage extended Kalman filter algorithm that can be used to estimate bias faults and loss of effectiveness for reaction flywheels in satellite attitude control systems. Zhang et al. [16–18] extended the two-stage method to CKF and proposed a two-stage CKF. This overcomes several problems faced by the augmented-state CKF, and solves high-dimensional nonlinear filter problems with minimal computational effort.

In the numerical simulation of solute transport in groundwater, there are unavoidable biases: the error of the model itself, the error in the field measurements, and the error in the solution process. To obtain better parameter values, identification results, and water quality prediction results, it is necessary to minimize the influence of these biases.

The Kalman filter algorithm essentially estimates the minimum variance in the state space. During the data processing stage, Kalman filters have high computational complexity. The two-stage Kalman filter algorithm can be applied to nonlinear systems with unknown random bias in order to estimate the high-dimensional state and process the measurement values. When applied to the identification of water quality parameters, the main task is to find the state equations and observation equations. The state equation describes the variation of the estimated value (the parameter to be considered) between the current time step and the next; the observation equation describes the relation between the estimated value and the actual observed value. Through "prediction correction," the optimal parameter values are obtained.

2. Determination of water pollution model

2.1. Determination of state equation

It is assumed that hydrogeological conditions in the study area remain stable. The horizontal and vertical dispersion coefficients, seepage velocity, and nitrification/denitrification coefficients also remain unchanged. The model parameter of solute transport is regarded as the state vector, and the observed solute concentration is regarded as the observation vector of the system. Thus, the corresponding state equation is:

$$x_{k+1} = f\left(x_k\right) + D_k b_k + \omega_k^x \tag{1(a)}$$

where $x_{k+1} = (D_x, D_y, u_x, u_y, q_s, R, 1)$ is the unknown parameter vector to be identified. The nonlinear function $f(\cdot)$ is the state transition function. The noise sequence ω_k^x is the zero-mean uncorrelated Gaussian random sequence.

The error of the model itself, the error in the field measurements, and the error in the solution process mean that the model has some unavoidable bias. The bias equation is:

$$b_{k+1} = b_k + \omega_k^b \tag{1(b)}$$

where the noise sequence ω_k^b is the zero-mean uncorrelated Gaussian random sequence.

2.2. Determination of observation equation

Consider the following solute transport equation:

$$\frac{\partial C}{\partial t} = D_x \frac{\partial^2 C}{\partial x^2} + D_y \frac{\partial^2 C}{\partial y^2} - u_x \frac{\partial C}{\partial x} - u_y \frac{\partial C}{\partial y} - q_s C + RC$$

where D_x, D_y are dispersion coefficients in the X and Y directions, respectively; u_x, u_y are the seepage velocities in the X and Y directions, respectively; q_s represents the source and sink term; R represents the coefficient of decay reaction; and C represents the concentration of contaminants.

The equation of solute transport in a groundwater system is nonlinear, and so a CKF can be used to solve the problem. The observation equation is:

$$z_k = h\left(x_k\right) + F_k b_k + \upsilon_k \tag{1(c)}$$

where the nonlinear function $h(\cdot)$ is the observation transition function. The noise sequence υ_k is a zero-mean uncorrelated Gaussian random sequence.

The noise sequences ω_k^x, ω_k^b, and υ_k are such that

$$E\left[\begin{bmatrix}\omega_k^x\\ \omega_k^b\\ \upsilon_k\end{bmatrix}\begin{bmatrix}\omega_j^x\\ \omega_j^b\\ \upsilon_j\end{bmatrix}^T\right] = \begin{bmatrix}Q_k^x & 0 & 0\\ 0 & Q_k^b & 0\\ 0 & 0 & R_k\end{bmatrix}\delta_{kj} \tag{2}$$

where $Q_k^x > 0, Q_k^b > 0, R_k > 0$, and δ_{kj} is the Kronecker's delta. The initial states x_0 and b_0 are assumed to be uncorrelated with the white noise processes ω_k^x, ω_k^b, and υ_k. We assume that the initial conditions x_0 and b_0 are Gaussian random variables with

$$E\left[x_0\right] = \bar{x}_0, E\left[(x_0 - \bar{x}_0)(x_0 - \bar{x}_0)^T\right] = P_0^x > 0$$

$$E\left[b_0\right] = \bar{b}_0, E\left[(b_0 - \bar{b}_0)(b_0 - \bar{b}_0)^T\right] = P_0^b > 0$$

$$E\left[(x_0 - \bar{x}_0)(b_0 - \bar{b}_0)^T\right] = P_0^{xb} > 0$$

3. Augmented-state cubature Kalman filter

Define

$$X_{k+1} = \begin{bmatrix}x_{k+1}\\ b_{k+1}\end{bmatrix}, f\left(X_k\right) = \begin{bmatrix}f\left(x_k\right) + D_k b_k\\ b_k\end{bmatrix}, \omega_k = \begin{bmatrix}\omega_k^x\\ \omega_k^b\end{bmatrix}$$
$$h\left(X_k\right) = h\left(x_k\right) + F_k b_k$$

The model given by Eqs. ((1) and 1(a)–(c)) can be rewritten as

$$X_{k+1} = f\left(X_k\right) + \omega_x \tag{3(a)}$$

$$Z_k = h\left(X_k\right) + \upsilon_k \tag{3(b)}$$

where

$$W = E\left(\omega_k \omega_j\right) = \begin{bmatrix} Q_k^x & 0 \\ 0 & Q_k^b \end{bmatrix} \delta_{kj}$$

Treating x_k and b_k as the augmented system state, the augmented-state CKF is described as follows.

3.1. Time update

(1) Assume that, at time k, the posterior density function $p\left(x_{k-1|k-1}\right) = \aleph(\hat{X}_{k-1|k-1}, P_{k-1|k-1})$ is known, and factorize

$$P_{k-1|k-1} = S_{k-1|k-1} S_{k-1|k-1}^T \tag{4}$$

(2) Evaluate the cubature points ($i = 1, 2, \cdots, m$)

$$X_{i,k-1|k-1} = S_{k-1|k-1}\xi_i + \hat{X}_{k-1|k-1} \tag{5}$$

(3) Evaluate the propagated cubature points ($i = 1, 2, \cdots, m$)

$$X^*_{i,k-1|k-1} = f(X_{i,k-1|k-1}, u_{k-1}) \tag{6}$$

(4) Estimate the predicted state

$$\hat{X}_{k|k-1} = \frac{1}{m}\sum_{i=1}^{m} X^*_{i,k-1|k-1} \tag{7}$$

(5) Estimate the predicted error covariance

$$P_{k|k-1} = \frac{1}{m}\sum_{i=1}^{m} X^*_{i,k-1|k-1} X^{*\,T}_{i,k-1|k-1} - \hat{X}_{k|k-1}\hat{X}_{k|k-1}^{\,T} + Q_{k-1} \tag{8}$$

3.2. Measurement update

Factorize

$$P_{k|k-1} = S_{k|k-1} S_{k|k-1}^T \tag{9}$$

(1) Evaluate the cubature points ($i = 1, 2, \cdots, m$)

$$X_{i,k|k-1} = S_{k|k-1}\xi_i + \hat{X}_{k|k-1} \tag{10}$$

(2) Evaluate the propagated cubature points ($i = 1, 2, \cdots, m$)

$$Z_{i,k|k-1} = h(X_{i,k|k-1}) \tag{11}$$

(3) Estimate the predicted state

$$\hat{Z}_{k|k-1} = \frac{1}{m}\sum_{i=1}^{m} Z_{i,k|k-1} \tag{12}$$

(4) Estimate the innovation covariance matrix

$$P_{zz,k|k-1} = \frac{1}{m}\sum_{i=1}^{m} Z_{i,k|k-1} Z_{i,k|k-1}^{\,T} - \hat{Z}_{k|k-1}\hat{Z}_{k|k-1}^{\,T} + R_k \tag{13}$$

(5) Estimate the cross-covariance matrix

$$P_{xz,k|k-1} = \frac{1}{m}\sum_{i=1}^{m} X_{i,k|k-1} Z_{i,k|k-1}^{\,T} - \hat{X}_{k|k-1}\hat{Z}_{k|k-1}^{\,T} \tag{14}$$

(6) Estimate the Kalman gain

$$K_k = P_{xz,k|k-1} P_{zz,k|k-1}^{-1} \tag{15}$$

(7) Estimate the updated state

$$\hat{X}_{k|k} = \hat{X}_{k|k-1} + K_k(Z_k - \hat{Z}_{k|k-1}) \tag{16}$$

(8) Estimate the corresponding error covariance

$$P_{k|k} = P_{k|k-1} - K_k P_{zz,k|k-1} K_k^T \tag{17}$$

The dimension of the above filter is $n+p$. When p is comparable to n, the dimension of the new state vector X_k becomes substantially larger than that of the initial system state, and the computational requirements of the augmented-state Kalman filter may become excessive. To overcome this problem, a large number of two-stage filter algorithms have been proposed. Although, the two-stage CKF (TSCKF) is optimal under an algebraic constraint, this constraint is too restrictive in practice, so TSCKF is usually suboptimal. In the next section, we describe a modified TSCKF that is equivalent to the augmented-state CKF.

4. Two-stage cubature Kalman filter

Theorem 1. Two-stage cubature Kalman filter
Let $\bar{X}^1_{k|k}$ be the output of the advancd bias-free filter:

$$\bar{X}^1_{k|k-1} = \frac{1}{m}\sum_{i=1}^{m} f^1\left(S_{k-1|k-1}\xi_i + T\left(\Psi, \bar{X}_{k-1|k-1}\right), u_{k-1}\right) - \Phi(\bar{X}^2_{k|k-1})$$

$$\bar{X}^1_{k|k} = \bar{X}^1_{k|k-1} + \Phi\left(\bar{X}^2_{k|k-1}\right) + V_k\left(\bar{X}^2_{k|k} - \bar{X}^2_{k|k-1}\right) - \Psi\left(\bar{X}^2_{k|k}\right) + \bar{K}^1_k\left(Z_k - \frac{1}{m}\sum_{i=1}^{m} h\left(S_{k|k-1}\xi_i + T\left(\Phi, \bar{X}_{k|k-1}\right), u_k\right)\right)$$

$$\bar{P}^1_{k|k-1} = M^{11}_{k-1} + Q^{11}_{k-1} - U_k (M^{12}_{k-1} + Q^{12}_{k-1})^T$$

$$\bar{P}^1_{k|k} = \bar{P}^1_{k|k-1} + U_k \bar{P}^2_{k|k-1} U^T_k - V_k \bar{P}^2_{k|k-1} V^T_k - \bar{K}^1_k P_{zz,k|k-1} \left(\bar{K}^1_k\right)^T - \bar{K}^1_k P_{zz,k|k-1} \left(\bar{K}^2_k\right)^T V^T_k - (\bar{K}^1_k P_{zz,k|k-1} \left(\bar{K}^2_k\right)^T V^T_k)^T$$

$$\bar{K}^1_k = N^1_k - V_k N^2_k$$

Let $\bar{X}^2_{k|k}$ be the output of the bias filter:

$$\bar{X}^2_{k|k-1} = \frac{1}{m} \sum_{i=1}^{m} f^2 \left(S_{k-1|k-1} \xi_i + T\left(\Psi, \bar{X}_{k-1|k-1}\right), u_{k-1}\right)$$

$$\bar{X}^2_{k|k} = \bar{X}^2_{k|k-1} + \bar{K}^2_k \left(Z_k - \frac{1}{m} \sum_{i=1}^{m} h\left(S_{k|k-1} \xi_i + T\left(\Phi, \bar{X}_{k|k-1}\right), u_k\right)\right)$$

$$\bar{P}^2_{k|k-1} = M^{22}_{k-1} + Q^{22}_{k-1}$$

$$\bar{P}^2_{k|k} = \bar{P}^2_{k|k-1} - \bar{K}^2_k P_{zz,k|k-1} \left(\bar{K}^2_k\right)^T$$

$$\bar{K}^2_k = N^2_k$$

The blending matrices U_k and V_k are given as follows:

$$U_k = (M^{12}_{k-1} + Q^{12}_{k-1})(M^{22}_{k-1} + Q^{22}_{k-1})^{-1}$$

$$V_k = U_k - \bar{K}^1_k P_{zz,k|k-1} \left(\bar{K}^2_k\right)^T (\bar{P}^2_{k|k-1})^{-1}$$

Proof. The key idea for our advanced TSCKF is based on the state transformations that make the covariance matrices block diagonal.

In linear systems, a two-stage Kalman filter can be obtained by the following T transformation:

$$T(G) = \begin{pmatrix} I_{n-p} & G \\ 0 & I_p \end{pmatrix} \tag{18}$$

Thus, using two-stage transformations, the CKF can be rewritten in the following form:

$$\hat{X}_{k|k-1} = T(U_k) \bar{X}_{k|k-1} \tag{19}$$

$$\hat{X}_{k|k} = T(V_k) \bar{X}_{k|k} \tag{20}$$

$$P_{k|k-1} = T(U_k) \bar{P}_{k|k-1} T^T(U_k) \tag{21}$$

$$P_{k|k} = T(V_k) \bar{P}_{k|k} T^T(V_k) \tag{22}$$

$$K_k = T(V_k) \bar{K}_k \tag{23}$$

where $\bar{P} = diag\{\bar{P}^1, \bar{P}^2\}$.

To extend the two-stage transformations to nonlinear systems, the T transformation of Eq. (18) is written as:

$$T\left(F, X\right) = \begin{bmatrix} X_1 + F(X_2) \\ X_2 \end{bmatrix} \tag{24}$$

where X = $\{(X^1)^T, (X^2)^T\}^T$, $X^1 \in R^{n-p}$ and $X^2 \in R^p$, and $F(X^2)$ is the nonlinear function of the substate X^2.

From Eq. (24), we can infer the following properties:

$$\frac{\partial T(\Phi, \bar{X}_{k|k-1})}{\partial \bar{X}_{k|k-1}} = \begin{bmatrix} I_{n-p} & U_k \\ 0 & I_p \end{bmatrix} \equiv T\left(U_k\right) \tag{25}$$

$$\frac{\partial T(\Psi, \bar{X}_{k|k})}{\partial \bar{X}_{k|k}} = \begin{bmatrix} I_{n-p} & V_k \\ 0 & I_p \end{bmatrix} \equiv T\left(V_k\right) \tag{26}$$

where

$$U_k = \frac{\partial \Phi(\bar{X}^2_{k|k-1})}{\partial \bar{X}^2_{k|k-1}}, V_k = \frac{\partial \Psi(\bar{X}^2_{k|k})}{\partial \bar{X}^2_{k|k}} \tag{27}$$

Using the T transformation with Eq. (24), the two-stage transformation Eqs. (19)–(23) becomes

$$\hat{X}_{k|k-1} = T(\Phi, \bar{X}_{k|k-1}) \tag{28}$$

$$\hat{X}_{k|k} = T(\Psi, \bar{X}_{k|k}) \tag{29}$$

$$P_{k|k-1} = \frac{\partial T\left(\Phi, \bar{X}_{k|k-1}\right)}{\partial \bar{X}_{k|k-1}} \bar{P}_{k|k-1} \left(\frac{\partial T(\Phi, \bar{X}_{k|k-1})}{\partial \bar{X}_{k|k-1}}\right)^T \tag{30}$$

$$P_{k|k} = \frac{\partial T\left(\Psi, \bar{X}_{k|k}\right)}{\partial \bar{X}_{k|k}} \bar{P}_{k|k-1} \left(\frac{\partial T(\Psi, \bar{X}_{k|k})}{\partial \bar{X}_{k|k}}\right)^T \tag{31}$$

$$K_k = \frac{\partial T\left(\Psi, \bar{X}_{k|k}\right)}{\partial \bar{X}_{k|k}} \bar{K}_k \tag{32}$$

where Φ and Ψ are given nonlinear functions.

Next, based on Eqs. (28)–(32), the improved TSCKF can be obtained via the following method.

In the first step, substitute Eqs. (7) and (16) into the left-hand side of Eqs. (28) and (29) such that, using Eq. (24), we obtain:

$$\begin{bmatrix} \bar{X}^1_{k|k-1} + \Phi(\bar{X}^2_{k|k-1}) \\ \bar{X}^2_{k|k-1} \end{bmatrix} = \frac{1}{m}\sum_{i=1}^{m} f\left(S_{k-1|k-1}\xi_i + T\left(\Psi, \bar{X}_{k-1|k-1}\right), u_{k-1}\right) \quad (33)$$

$$\begin{aligned} \begin{bmatrix} \bar{X}^1_{k|k} + \Psi\left(\bar{X}^2_{k|k}\right) \\ \bar{X}^2_{k|k} \end{bmatrix} &= \begin{bmatrix} \bar{X}^1_{k|k-1} + \Phi\left(\bar{X}^2_{k|k-1}\right) \\ \bar{X}^2_{k|k-1} \end{bmatrix} \\ &+ K_k\left(Z_k - \frac{1}{m}\sum_{i=1}^{m} h\left(S_{k|k-1}\xi_i + T\left(\Phi, \bar{X}_{k|k-1}\right), u_k\right)\right) \end{aligned} \quad (34)$$

Expanding Eqs. (33) and (34) and using Eqs. (26) and (32) gives:

$$\begin{aligned} \bar{X}^1_{k|k-1} &= \frac{1}{m}\sum_{i=1}^{m} f^1\left(S_{k-1|k-1}\xi_i + T\left(\Psi, \bar{X}_{k-1|k-1}\right), u_{k-1}\right) \\ &- \Phi\left(\bar{X}^2_{k|k-1}\right) \end{aligned} \quad (35)$$

$$\begin{aligned} \bar{X}^1_{k|k} &= \bar{X}^1_{k|k-1} + \Phi\left(\bar{X}^2_{k|k-1}\right) + V_k\left(\bar{X}^2_{k|k} - \bar{X}^2_{k|k-1}\right) - \Psi\left(\bar{X}^2_{k|k}\right) \\ &+ \bar{K}^1_k\left(Z_k - \frac{1}{m}\sum_{i=1}^{m} h\left(S_{k|k-1}\xi_i + T\left(\Phi, \bar{X}_{k|k-1}\right), u_k\right)\right) \end{aligned} \quad (36)$$

$$\bar{X}^2_{k|k-1} = \frac{1}{m}\sum_{i=1}^{m} f^2\left(S_{k-1|k-1}\xi_i + T\left(\Psi, \bar{X}_{k-1|k-1}\right), u_{k-1}\right) \quad (37)$$

$$\bar{X}^2_{k|k} = \bar{X}^2_{k|k-1} + \bar{K}^2_k\left(Z_k - \frac{1}{m}\sum_{i=1}^{m} h\left(S_{k|k-1}\xi_i + T\left(\Phi, \bar{X}_{k|k-1}\right), u_k\right)\right) \quad (38)$$

where

$$f(\cdot) = \left[\left(f^1(\cdot)\right)^T \quad \left(f^2(\cdot)\right)^T\right]^T$$

$$\bar{K}_k = \left[\left(\bar{K}^1_k\right)^T \quad \left(\bar{K}^2_k\right)^T\right]^T$$

According to Eq. (8), we can write:

$$M_{k-1} = \frac{1}{m}\sum_{i=1}^{m} X^*_{i,k-1|k-1}\sum_{i=1}^{m} X^*_{i,k-1|k-1}{}^T - \hat{X}_{k|k-1}\hat{X}_{k|k-1}{}^T \quad (39)$$

which can be written in matrix form as:

$$M_{k-1} = \begin{bmatrix} M^{11}_{k-1} & M^{12}_{k-1} \\ \left(M^{12}_{k-1}\right)^T & M^{22}_{k-1} \end{bmatrix} \quad (40)$$

and then:

$$P_{k|k-1} = M_{k-1} + Q_{k-1} = \begin{bmatrix} M^{11}_{k-1} + Q^{11}_{k-1} & M^{12}_{k-1} + Q^{12}_{k-1} \\ \left(M^{12}_{k-1} + Q^{12}_{k-1}\right)^T & M^{22}_{k-1} + Q^{22}_{k-1} \end{bmatrix} \quad (41)$$

Using Eqs. (25) and (30) then yields:

$$\bar{P}^1_{k|k-1} = M^{11}_{k-1} + Q^{11}_{k-1} - U_k(M^{12}_{k-1} + Q^{12}_{k-1})^T \quad (42)$$

$$\bar{P}^2_{k|k-1} = M^{22}_{k-1} + Q^{22}_{k-1} \quad (43)$$

$$U_k = (M^{12}_{k-1} + Q^{12}_{k-1})(M^{22}_{k-1} + Q^{22}_{k-1})^{-1} \quad (44)$$

Expanding the transformation Eq. (31) using Eqs. (30) and (32) gives:

$$\begin{aligned} \bar{P}^1_{k|k} &= \bar{P}^1_{k|k-1} + U_k\bar{P}^2_{k|k-1}U^T_k - V_k\bar{P}^2_{k|k-1}V^T_k - \bar{K}^1_k P_{zz,k|k-1}\left(\bar{K}^1_k\right)^T \\ &- \bar{K}^1_k P_{zz,k|k-1}\left(\bar{K}^2_k\right)^T V^T_k - \left(\bar{K}^1_k P_{zz,k|k-1}\left(\bar{K}^2_k\right)^T V^T_k\right)^T \end{aligned} \quad (45)$$

$$\bar{P}^2_{k|k} = \bar{P}^2_{k|k-1} - \bar{K}^2_k P_{zz,k|k-1}\left(\bar{K}^2_k\right)^T \quad (46)$$

$$V_k = U_k - \bar{K}^1_k P_{zz,k|k-1}\left(\bar{K}^2_k\right)^T (\bar{P}^2_{k|k-1})^{-1} \quad (47)$$

According to Eqs. (13)–(15), writing

$$N_k = P_{xz,k|k-1}P^{-1}_{zz,k|k-1} \quad (48)$$

gives

$$K_k = N_k = \begin{bmatrix} N^1_k \\ N^2_k \end{bmatrix} \quad (49)$$

and using Eq. (29), we deduce that:

$$\bar{K}^1_k = N^1_k - V_k N^2_k \quad (50)$$

$$\bar{K}^2_k = N^2_k \quad (51)$$

This completes the proof.

The problem of obtaining Φ and Ψ remains. This can be solved using Eq. (32) and the backward difference equation as follows:

$$\Phi(\bar{X}^2_{k|k-1}) = \Phi(\bar{X}^2_{k-1|k-2}) + U_k(\bar{X}^2_{k|k-1} - \bar{X}^2_{k-1|k-2})$$

$$\Psi(\bar{X}^2_{k|k}) = \Psi(\bar{X}^2_{k-1|k-1}) + V_k(\bar{X}^2_{k|k} - \bar{X}^2_{k-1|k-1})$$

5. Equivalence proof of two-stage cubature Kalman filter

The TSCKF algorithm is obtained by a nonsingular two-stage transformation of the CKF algorithm, so their equivalence can be proved mathematically.

Theorem 1. The TSCKF algorithm is equivalent to the CKF algorithm.

Proof. By inductive reasoning, suppose that, at time *k*:

$$\hat{X}_{k|k} = X_{k|k} \quad (52)$$

Then, by Eqs. (5)–(7), (24), (35)–(37) and (52), we have that:

$$T\left(\phi,\bar{X}_{k+1|k}\right)=\begin{pmatrix}\bar{X}^1_{k+1|k}+\phi\left(\bar{X}^2_{k+1|k}\right)\\ \bar{X}^2_{k+1|k}\end{pmatrix}=\frac{1}{m}\sum_{i=1}^{m}f\left(S_{k|k}\xi_i+T\left(\psi,\bar{X}_{k|k}\right),u_k\right)$$
$$=\frac{1}{m}\sum_{i=1}^{m}f(S_{k|k}\xi_i+\hat{X}_{k|k},u_k)=X_{k+1|k} \tag{53}$$

Eqs. (16), (29), (32), (38), (49) and (53) gives

$$\hat{X}_{k+1|k+1}=$$
$$\begin{bmatrix}\bar{X}^1_{k+1|k}+\Phi\left(\bar{X}^2_{k+1|k}\right)+V_k\left(\bar{X}^2_{k+1|k+1}-\bar{X}^2_{k+1|k}\right)+\bar{K}^1_{k+1}\left(Z_{k+1}-\frac{1}{m}\sum_{i=1}^{m}h\left(S_{k+1|k}\xi_i+T\left(\Phi,\bar{X}_{k+1|k}\right),u_{k+1}\right)\right)\\ \bar{X}^2_{k+1|k}+\bar{K}^2_{k+1}\left(Z_{k+1}-\frac{1}{m}\sum_{i=1}^{m}h\left(S_{k+1|k}\xi_i+T\left(\Phi,\bar{X}_{k+1|k}\right),u_{k+1}\right)\right)\end{bmatrix}$$
$$=T\left(\phi,\bar{X}_{k+1|k}\right)+\begin{bmatrix}\bar{K}^1_{k+1}\\ \bar{K}^2_{k+1}\end{bmatrix}\left(Z_{k+1}-\hat{Z}_{k+1|k}\right)+\begin{bmatrix}V_{k+1}\left(\bar{X}^2_{k+1|k+1}-\bar{X}^2_{k+1|k}\right)\\ 0\end{bmatrix}$$
$$=T\left(\phi,\bar{X}_{k+1|k}\right)+\begin{bmatrix}\bar{K}^1_{k+1}+V_{k+1}\bar{K}^2_{k+1}\\ \bar{K}^2_{k+1}\end{bmatrix}\left(Z_{k+1}-\hat{Z}_{k+1|k}\right)$$
$$=X_{k+1|k}+K_{k+1}\left(Z_{k+1}-\hat{Z}_{k+1|k}\right)=X_{k+1|k+1} \tag{54}$$

According to Eq. (54), the expression in Eq. (52) is also true at time k+1.

This completes the proof.

6. Simulation examples

6.1. Experiment to demonstrate the effectiveness of the TSCKF algorithm

The true value and estimated value of the dispersion coefficients along the X and Y directions, the seepage velocity along the X and Y directions, and the source and sink term are illustrated in Figs. 1–10 alongisde the estimation error.

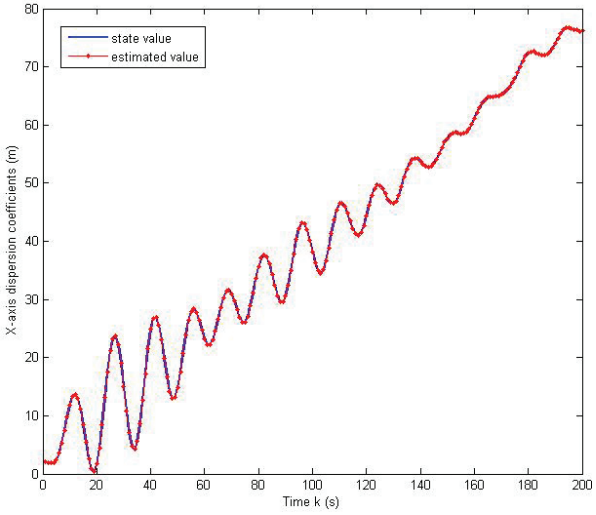

Fig. 1. X-axis dispersion coefficients.

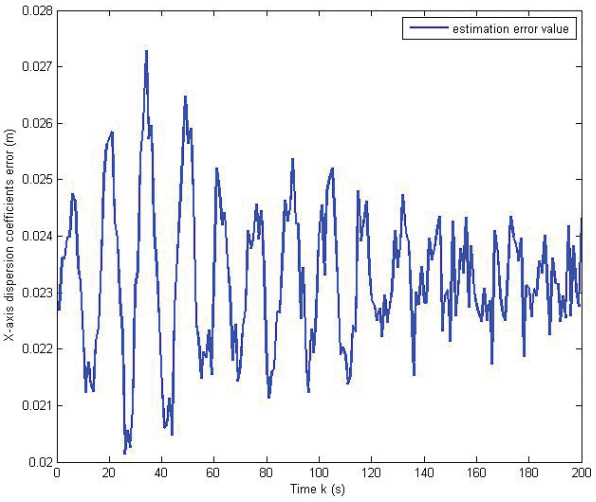

Fig. 2. X-axis dispersion coefficients error.

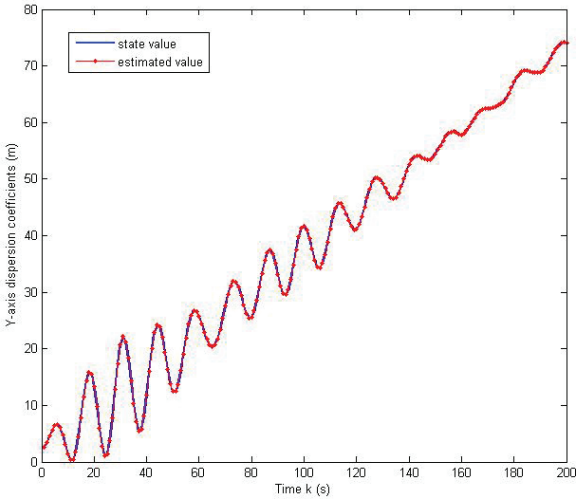

Fig. 3. Y-axis dispersion coefficients.

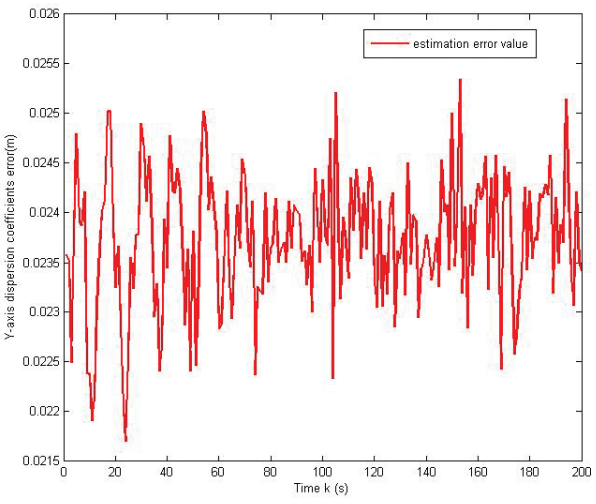

Fig. 4. Y-axis dispersion coefficients error.

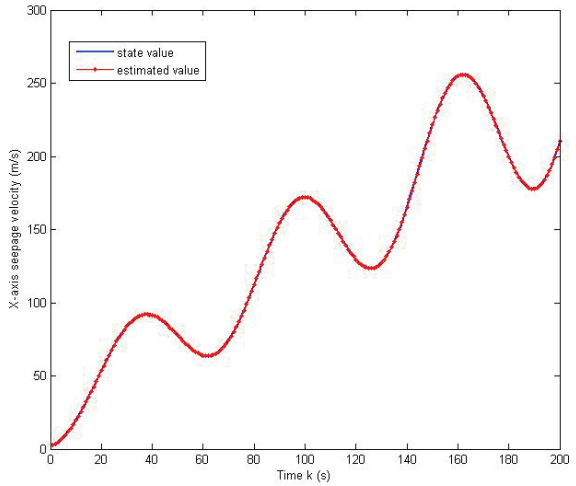

Fig. 5. X-axis seepage velocity.

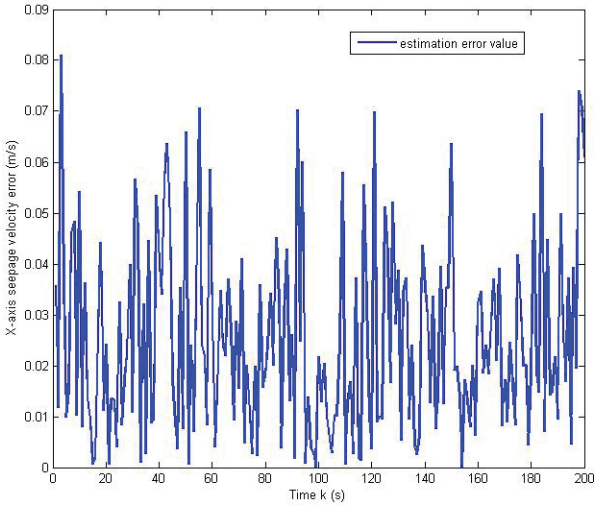

Fig. 6. X-axis seepage velocity error.

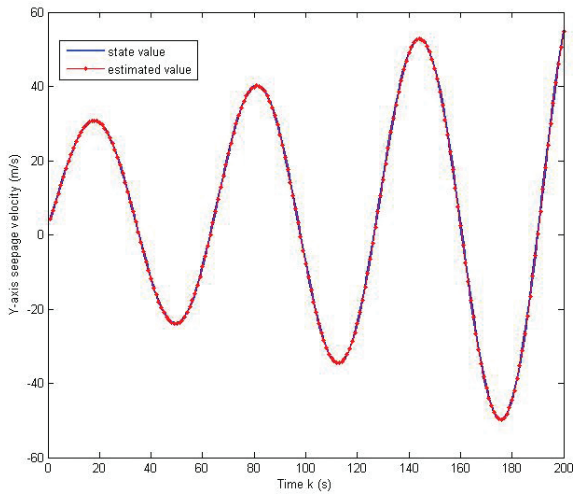

Fig. 7. Y-axis seepage velocity.

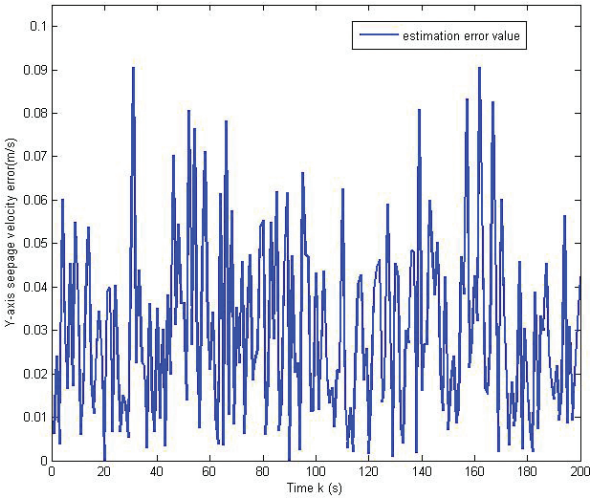

Fig. 8. Y-axis seepage velocity error.

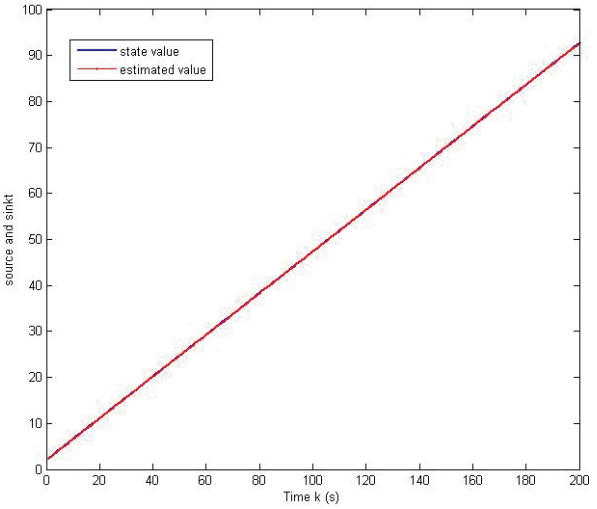

Fig. 9. Source and sinkt.

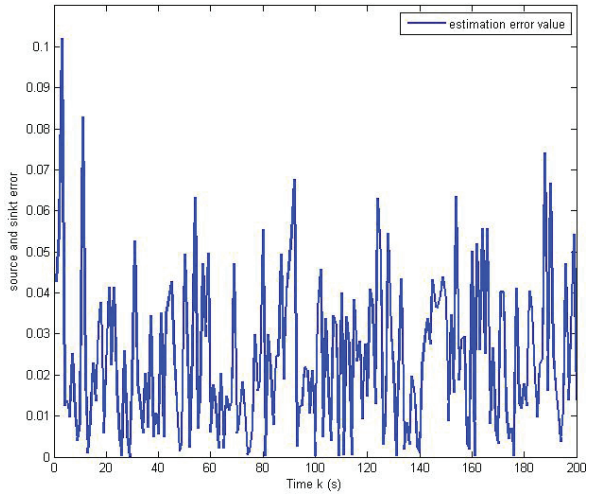

Fig. 10. Source and sinkt error.

It can be seen from Figs. 2, 4, 6, 8, and 10 that the estimated error is within a small range that can be neglected in practical applications. In fact, this error is caused by the numerical method of solution. Therefore, the estimate given by TSCKF is the same as the state value, and the estimation results can be accepted.

Figs. 11 and 12 show the bias value and bias error value. The state values are derived from the augmented-state computation and the estimated values are derived from TSCKF. As in the previous estimated error figures, the bias error are within a small range and the estimated value of the bias is similar to the bias state value.

6.2 Comparison between CKF and TSCKF algorithm

Using the same simulation model as described in section 6.1 and a simulation time of 200 s, 1000 Monte Carlo simulations of the TSCKF algorithm were carried out.

Figs. 13, 15, 17, 19, and 21 compare the state estimates between the CKF and TSCKF algorithms. From these figures,

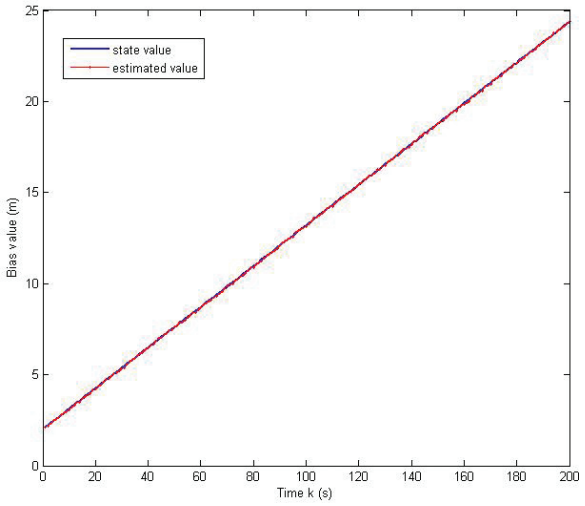

Fig. 11. Bias value.

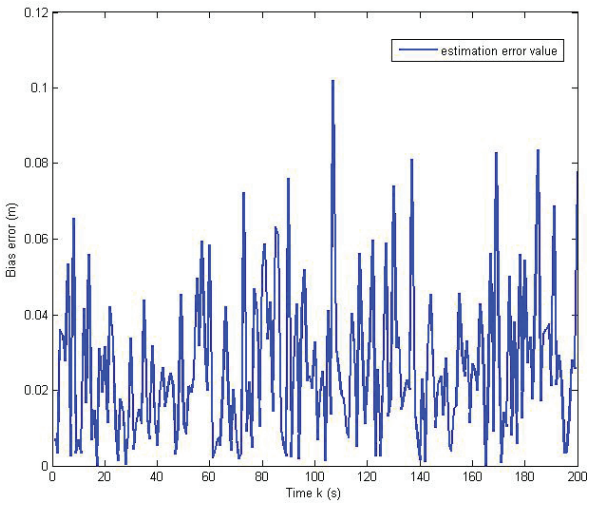

Fig. 12. Bias error.

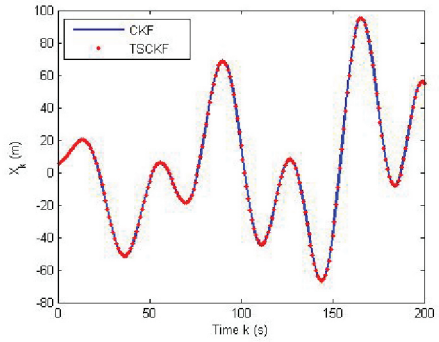

Fig. 13. Comparison of two algorithms for X_k estimation.

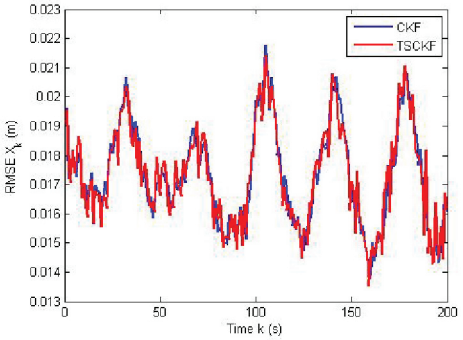

Fig. 14. Comparison of RMSE of two algorithms for X_k estimation.

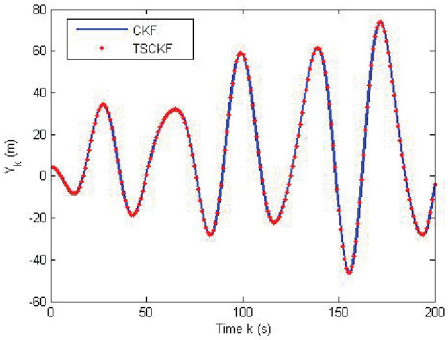

Fig. 15. Comparison of two algorithms for Y_k estimation.

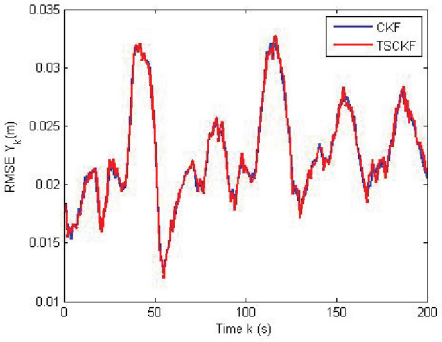

Fig. 16. Comparison of RMSE of two algorithms for Y_k estimation.

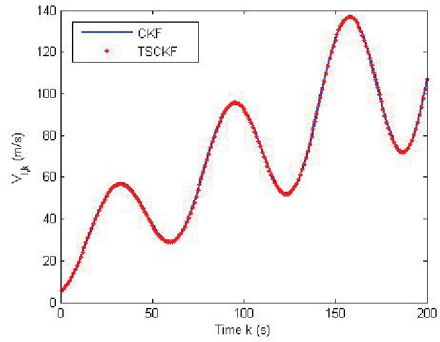

Fig. 17. Comparison of two algorithms for $V_{l,k}$ estimation.

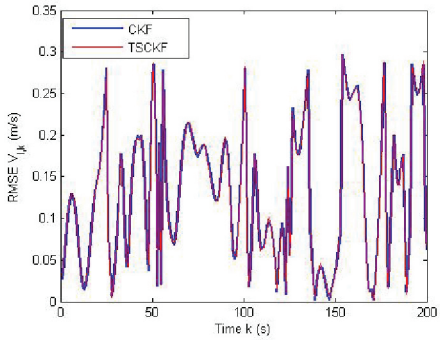

Fig. 18. Comparison of RMSE of two algorithms for $V_{l,k}$ estimation.

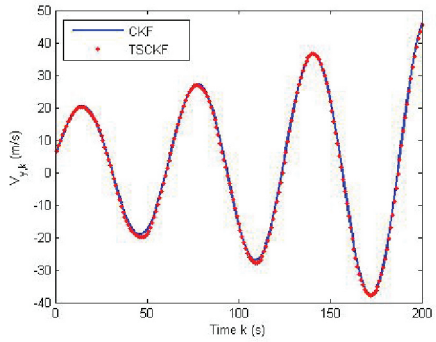

Fig. 19. Comparison of two algorithms for $V_{y,k}$ estimation.

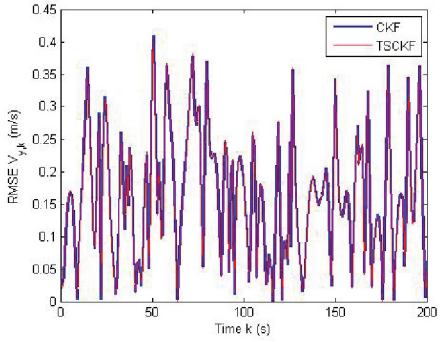

Fig. 20. Comparison of RMSE of two algorithms for $V_{y,k}$ estimation.

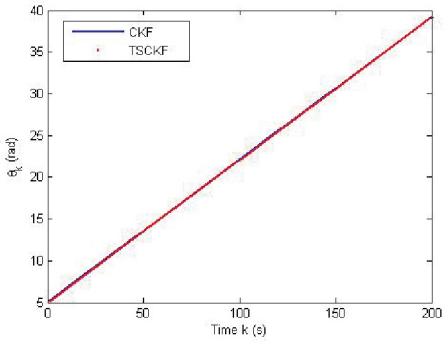

Fig. 21. Comparison of two algorithms for θ_k estimation.

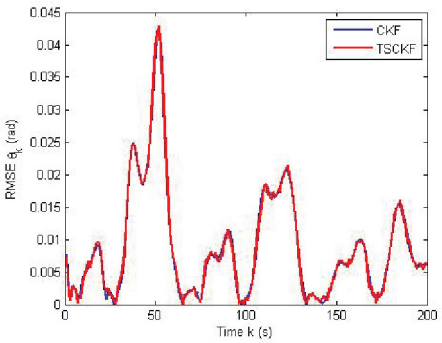

Fig. 22. Comparison of RMSE of two algorithms for θ_k estimation.

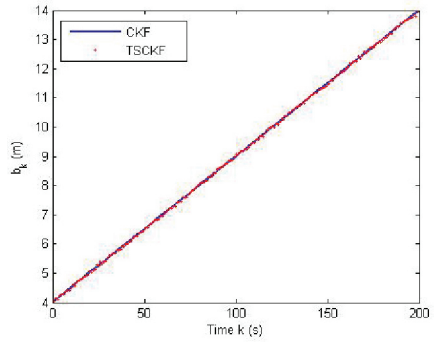

Fig. 23. Comparison of two algorithms for b_k estimation.

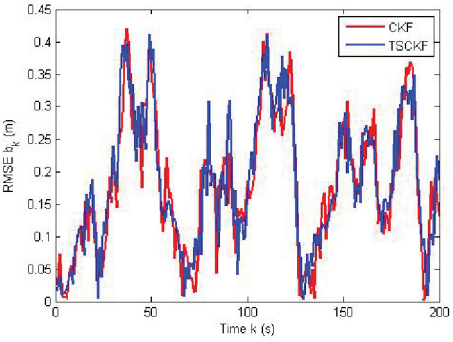

Fig. 24. Comparison of RMSE of two algorithms for b_k estimation.

we can see that the two algorithms give similar estimated values of the state vector, which proves the applicability of the TSCKF algorithm. Figs. 14, 16, 18, 20, and 22 compare the root mean square error (RMSE) between the CKF and TSCKF algorithms. From these figures, it is clear that the accuracy of the two algorithms is comparable, which proves the equivalence of the two algorithms.

Fig. 23 compares the deviation vector b_k of the estimates given by the two algorithms. Fig. 24 compares the RSME of the deviation vector b_k. As can be seen from these figures, the RMSE of the two algorithms is equal, which demonstrates the equivalence of the two algorithms.

7. Conclusion

This paper has described a two-stage cubature Kalman filter for water pollution models, which are nonlinear systems with random bias. Our TSCKF is equivalent to the augmented-state CKF and provides optimal results. The simulation results demonstrate the validity of the TSCKF algorithm and prove the equivalence with the augmented-state CKF algorithm.

Acknowledgments

This work was partially supported by the National Nature Science Fund of China (NSFC) (Grant No. 61503213) and Zhejiang Natural Science Foundation Project (Grant No. LY15F020041). We thank Stuart Jenkinson, PhD, for editing the English text of a draft of this manuscript.

References

[1] B. Friedland, Treatment of bias in recursive filtering, IEEE. Trans. Autom. Control., 14 (1969) 359–367.
[2] A.T. Alouani, P. Xia, T.R. Rice, W.D. Blair, On the Optimality of Two-Stage State Estimation In the Presence of Random Bias, IEEE. Trans. Autom. Control, 38 (1993) 1279–1282.
[3] C.S. Hsieh, F.C. Chen, Optimal solution of the two-stage Kalman estimator, IEEE. Trans. Autom. Control., 44 (1999) 194–199.
[4] J.Y. Keller, M. Darouach, Optimal two-stage Kalman filter in the presence of random bias, Automatica, 33 (1997) 1745–1748.
[5] C.S. Hsieh, F.C. Chen, General two-stage Kalman filters, IEEE. Trans. Autom. Control., 48 (2000) 819–824.
[6] C.B. Wen, Z.D. Wang, Q.Y. Liu, F.E. Alsaadi, Recursive distributed filtering for a class of state-saturated systems with fading measurements and quantization effects, IEEE. Trans. Syst. Man. Cybern. Syst., 48 (2018) 930–941.
[7] Q.B. Ge, D.X. Xu, C.L. Wen, Cubature information filters with correlated noises and their applications in decentralized fusion, Signal. Process., 94 (2014) 434–444.
[8] Q.B. Ge, C.L. Wen, S.D. Chen, Cubature Kalman fusion for bearings only tracking networks. 3rd IFAC International Conference on Intelligent Control and Automation Science, Chengdu, China, 2013.
[9] C.S. Hsieh, General Two-Stage Extended Kalman Filters, IEEE. Trans. Autom. Control., 48 (2003) 289–293.
[10] Y.G. Zhang, Y.L. Huang, N. Li, L. Zhao, Embedded cubature Kalman filter with adaptive setting of free parameter, Signal. Process., 114 (2015) 112–116.
[11] Y.G. Zhang, Y.L. Huang, N. Li, L. Zhao, Interpolatory cubature Kalman filters, Control. Theory. Appl. Iet., 9 (2015) 1731–1739.
[12] Y.G. Zhang, Y.L. Huang, N. Li, L. Zhao, A high order unscented Kalman filtering method, Acta. Automatica. Sinica., 40 (2014) 838–848.
[13] Y.G. Zhang, Y.L. Huang, N. Li, L. Zhao, Quasi-stochastic integration filter for nonlinear estimation, Math. Prob. Eng., (2014) 816–830.
[14] J.H. Xu, Y.W. Jing, G.M. Dinirovski, Two-stage unscented Kalman filter for nonlinear system in the presence of unknown random bias, American Control Conference, Washington, American, 2008, pp. 3530–3535.
[15] X.Q. Chen, R. Sun, W.C. Jiang, Q.X. Jia, J.X. Zhang, A novel two-stage extended Kalman filter algorithm for reaction flywheels fault estimation, Chinese. J. Aeronaut., 29 (2016) 462–469.
[16] L. Zhang, M.L. Lv, Z.Y. Niu, W.B. Rao, Two-Stage Cubature Kalman Filter for Nonlinear System with Random Bias. 2014 IEEE International Conference on Multisensory Fusion and Information (MFI 2014), Beijing, China, 2014, pp. 47–55.
[17] I. Arasaratnam, S. Haykin, Cubature Kalman Filters. IEEE Transactions on Automatic Control, 54 (2009) 1254–1269.
[18] L. Zhang, W.B. Rao, H.l. Wang, D.X. Xu, A Novel Two-stage Cubature Kalman Filter for Nonlinear System, J. Resid. Sci. Technol., 13 (2016) 206.1–206.8.